

Mid-infrared interferometry on spectral lines: I. Instrumentation

J. D. Monnier¹, W. Fitelson, W. C. Danchi² and C. H. Townes

Space Sciences Laboratory, University of California, Berkeley, Berkeley, CA 94720-7450

ABSTRACT

The U. C. Berkeley Infrared Spatial Interferometer has been outfitted with a filterbank system to allow interferometric observations of mid-infrared spectral lines with very high spectral resolution ($\frac{\lambda}{\Delta\lambda} \sim 10^5$). This paper describes the design, implementation, and performance of the matched 32-channel filterbank modules, and new spectral line observations of Mars and IRC +10216 are used to demonstrate their scientific capability. In addition, observing strategies are discussed for accurate calibration of fringe visibilities in spectral lines, despite strong atmospheric fluctuations encountered in the infrared.

Subject headings: instrumentation: interferometers, instrumentation: spectrographs, techniques: interferometric

1. Introduction

The Infrared Spatial Interferometer (ISI) consists of two 1.65-m telescopes employing heterodyne detection between 9–12 μm using CO₂ lasers as local oscillators (LO) (Hale et al. 2000; Lipman 1998). Observations can be made at a large number of frequency bands in this spectral range by tuning to the various lasing transitions of different CO₂ isotopes. The ISI has measured the characteristics (sizes and optical depths) of dust shells around late-type stars (e.g., Danchi et al. 1994) and angular diameters of the nearest red supergiants (Bester et al. 1996). In these cases, sensitivity to continuum (dust or photospheric) emission using heterodyne detection is generally less than that theoretically possible using direct (photon-counting) detection techniques, partly because the maximum bandpass is limited by the temporal response of the IR detector, which is about 5 GHz with present detectors ($\frac{\lambda}{\Delta\lambda} \sim 5000$).

However for narrow bandpasses, heterodyne receivers are more sensitive than direct detection schemes, which are not background-limited for low flux levels (see more detailed discussion by Monnier [1999] and Hale *et al.* [2000]). Furthermore, extremely high spectral resolution is attainable

¹Current Address: Smithsonian Astrophysical Observatory MS#42, 60 Garden Street, Cambridge, MA, 02138

²Current Address: NASA Goddard Space Flight Center, Infrared Astrophysics, Code 685, Greenbelt, MD 20771

with heterodyne spectroscopy (e.g., Betz 1977) since the down-converted astronomical signal can be further filtered with conventional radio-frequency (RF) filters. Such high resolution is needed to resolve many molecular lines which form in cool winds around AGB stars ($\Delta v \sim 1 \text{ km s}^{-1}$) or in planetary atmospheres. Betz was able to observe transitions of CO_2 around Mars and Venus with spectral resolution of $\frac{\lambda}{\Delta\lambda} \sim 6 \times 10^6$ (Betz et al. 1976). Interferometry with this resolution can hence measure the location and distribution of molecules in particular excitation states.

Naturally, the high spectral resolution potential of a heterodyne system can only be realized by using a spectrometer in the RF signal chain following detection, a capability not part of the original ISI design. Although previous systems have been built for high efficiency spectral line work with wide RF bandwidths on single telescopes (e.g., Betz 1977; Goldhaber 1988; Isaak, Harris & Zmuidzinas 1999; Holler 1999), no system existed that was suitable for interferometry on narrow bands because of the need to correlate signals from two separate telescopes.

This paper will describe the implementation of an inexpensive filterbank system for spectral line observations using the ISI. After a description of the filterbank itself, its performance will be evaluated from laboratory measurements and test observations of astronomical objects. Fluctuations from the turbulent atmosphere and unexpected instrumental drifts required new observing strategies for accurate calibration of the fringe visibility on and off of spectral lines. These techniques are described in detail, including fast bandpass switching for phase-referencing and LO-switching for robust correlator calibration. Lastly, the near-term scientific potential of combining high spectral and spatial resolution at these wavelengths is reviewed.

2. The 32-Channel Filterbank

2.1. Introduction

In principle, heterodyne spectroscopy with an RF filterbank is quite simple, even at 27 THz. A CO_2 laser in each ISI telescope acts as a local oscillator, with a wavelength of $\sim 11 \mu\text{m}$. Wavefronts from the laser are mixed with light from the sky and the resulting “beat” pattern is detected by a HgCdTe photoconductor with a large output bandwidth ($\pm \Delta\nu$). This process is called “heterodyne” detection and down-converts a $2\Delta\nu$ bandwidth centered around 27 THz (mid-infrared radiation) into microwave signals between DC and $\Delta\nu$. In a double-sideband (DSB) system such as the ISI, frequencies both above and below the local oscillator frequency are converted into the same (microwave) frequency, thus overlapping each other. When observing a spectral line, this has the undesired effect of diluting the line (in one sideband) with uninteresting continuum radiation (from the other sideband), but can still be readily interpreted when multiple spectral features are not overlapping.

Once the signals have been down-converted to microwave (or RF) frequencies, they are amplified by cold FET amplifiers and transmitted through coaxial cables. Tunable RF filters with band-

widths of 60 MHz (and much narrower) have been available for quite some time, and can be used to filter the astrophysical signals. Since the original frequency of the radiation was ~ 27 THz, the use of filters with 60 MHz bandwidth corresponds to a spectral resolving power of $\frac{\lambda}{\Delta\lambda} = \frac{27 \text{ THz}}{60 \text{ MHz}} = 4.5 \times 10^5$, fine enough to resolve spectral features arising from doppler shifts as small as $\sim 0.7 \text{ km s}^{-1}$.

2.2. Design Considerations

Being a first generation instrument, the design goals of the ISI filterbank were modest:

- Spectral resolution must be sufficient to resolve narrow absorption lines around AGB stars (a few km/s)
- Full bandpass must be broad enough to encompass both the relevant absorption line and significant bandwidth of continuum (~ 2 GHz)
- Due to high demand for ISI continuum observations, the filterbank system should minimally interfere with standard observing, i.e. should not involve a radically different hardware configuration
- A fast bandpass switching scheme to calibrate atmospheric fluctuations should be implemented
- Cost must be relatively low, – i.e., no digital correlator

Table 1 summarizes the technical features of the completed filterbank system, satisfying all of the above design goals. The desire to minimally impact the current hardware design of the ISI imposed the most severe restrictions on the design. In order to maintain the current RF architecture behind the correlator and to avoid the development of an entirely new data acquisition

Table 1: Important Specifications of ISI Filterbank

Bandpass	270-2190 MHz
Number of Filters	32 per telescope
Individual Filter Bandwidth (3dB points)	60 MHz
Spectral Resolution at $11.15 \mu\text{m}$	$\sim 0.7 \text{ km s}^{-1}$
Phase Matching	$\pm 10^\circ$ over 80% of band $\pm 20^\circ$ over entire band
Gain Dynamic Range	15 dB
Bandpass Switching Rate	up to 500 Hz

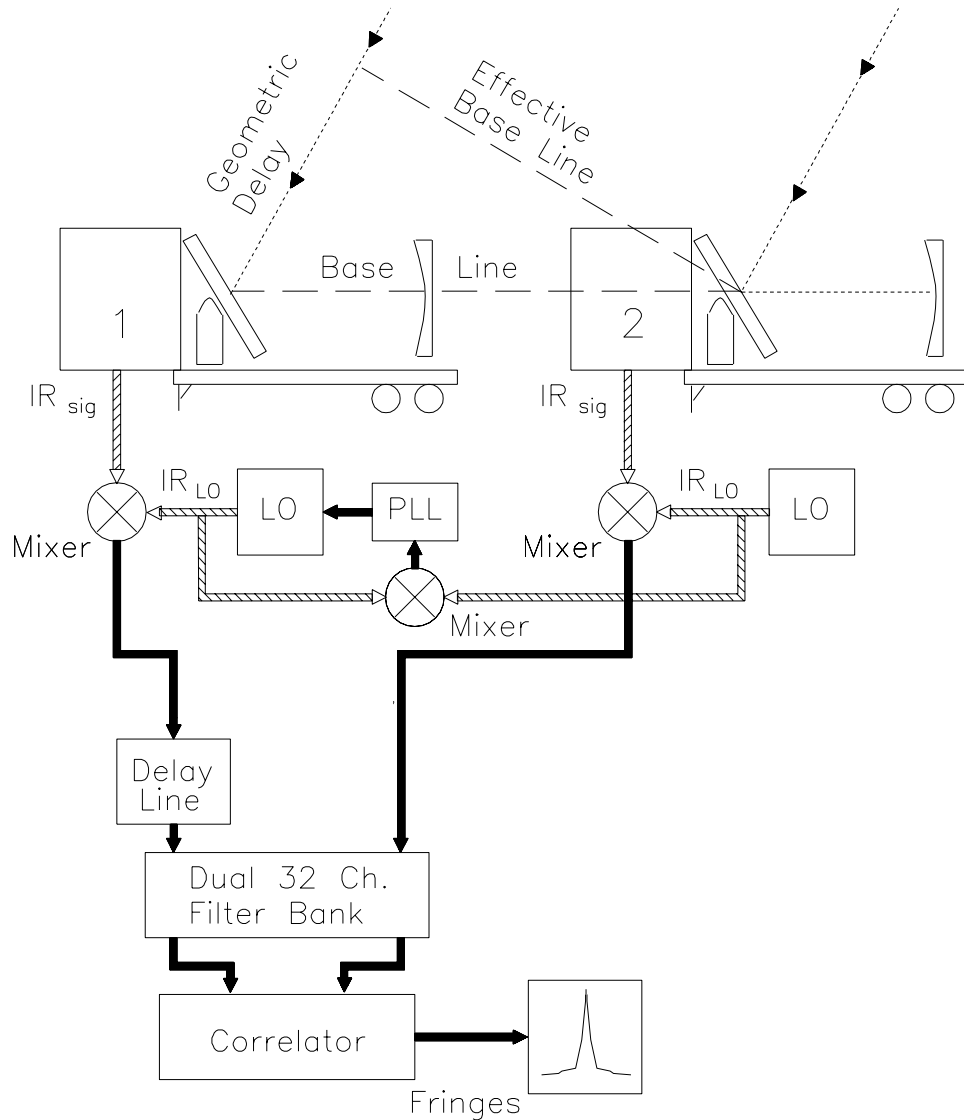


Fig. 1.— This figure shows a block diagram of the ISI interferometer with the filterbank in the RF path. Two trailers, each containing a telescope are indicated. Infrared (IR) signals are mixed with local oscillator (LO) power from CO₂ lasers. After passing through a filterbank which determines the bandpass, the resulting radio frequency (RF) signals from the two telescopes interfere in a correlator, producing interference fringes. The two LOs are kept in phase by a Phase Lock Loop (PLL) circuit. See Hale *et al.* (2000) for complete details.

system, spectroscopic capabilities were added to the ISI by inserting a filterbank system before the correlator and total infrared power detection subsystems. Figure 1 shows a schematic of the major subsystems of the Infrared Spatial Interferometer (ISI), including the dual 32-channel filterbank. Detailed descriptions of the ISI itself can be found in the instrument paper by Hale *et al.* (2000) and in recent PhD theses (Lipman 1998; Monnier 1999).

The interferometer must be able to measure not only the flux density of infrared radiation incident on both telescopes (i.e., the total IR power), but also the strength of the interference of signals from both telescopes (i.e., the fringe power). By filtering the RF signals from both telescopes with the two filterbank modules before correlation, the infrared (IR) power and fringe signal could be measured in a manner identical to that used for the broadband (continuum) signal. When not performing spectroscopic observations, the filterbank can be switched out of the RF path through a bypass line inside each filterbank module (see figure 2). This strategy has the distinct advantage of not impacting the existing hardware *at all*, and also does not require any additional RF detection or data acquisition development. However, because the filterbank intercepts the RF signals before correlation, the two modules of the filterbank (one set of 32 filters for each telescope) must be phase-matched. This imposed strict requirements on all the RF components inside the filterbank and contributed significantly to construction complexity and component costs. The other important performance trade-off was that only one filter bandpass can be observed at a time, unlike typical spectrometers where detectors (e.g., RF diodes) are placed behind all filters and read out in parallel, allowing the entire spectral line to be measured at once. This limits the uses of the filterbank, for example making it impractically slow to perform standard spectroscopic observations for a large number of lines.

Figure 2 shows a detailed block diagram of one of the two filterbank modules, with every major component in the RF chain. In order to filter the bandpass, the original RF signal from each telescope is split into 32 frequency bands via a 4-way power splitter followed by four 8-way splitters. This decreases the signal power in each band by 15 dB, and amplification is applied before, during, and after this splitting to keep signal levels high enough that the additional amplifier noise from this part of the signal chain causes no significant decrease to the signal-to-noise ratio (SNR). In addition, custom frequency equalizers are used to maintain a reasonably flat frequency response throughout each module and within each sub-module. After being split into 32 bands, the RF signals encounter the filters. Thirty-two switches are used to select the desired bandpass (any combination is allowed), after which the signals are recombined through a symmetric combination of four 8-way combiners and a single 4-way combiner. Following recombination, the signal is amplified and any overall bandpass slope removed before finally being re-injected into the ISI system.

In order to make sure that the filterbank puts out as much RF power as it receives (net power gain of 0 dB) independent of the bandpass selected, a variable attenuator and amplifier are used in combination to provide up to 15 dB of relative amplification. This is done so that the laser shot-noise always dominates the measurement noise, and that the final detection diodes are always used at similar power levels.

Filterbank Module

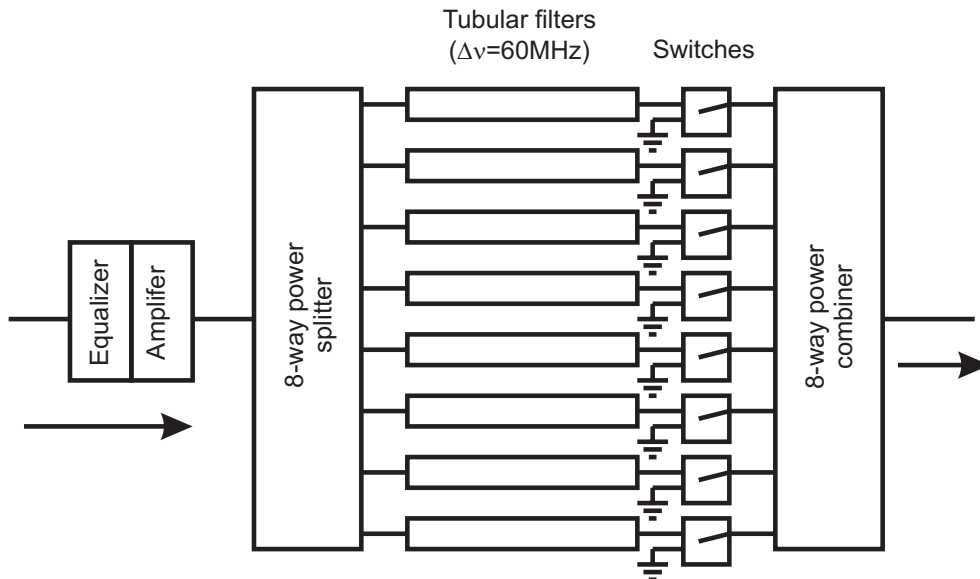
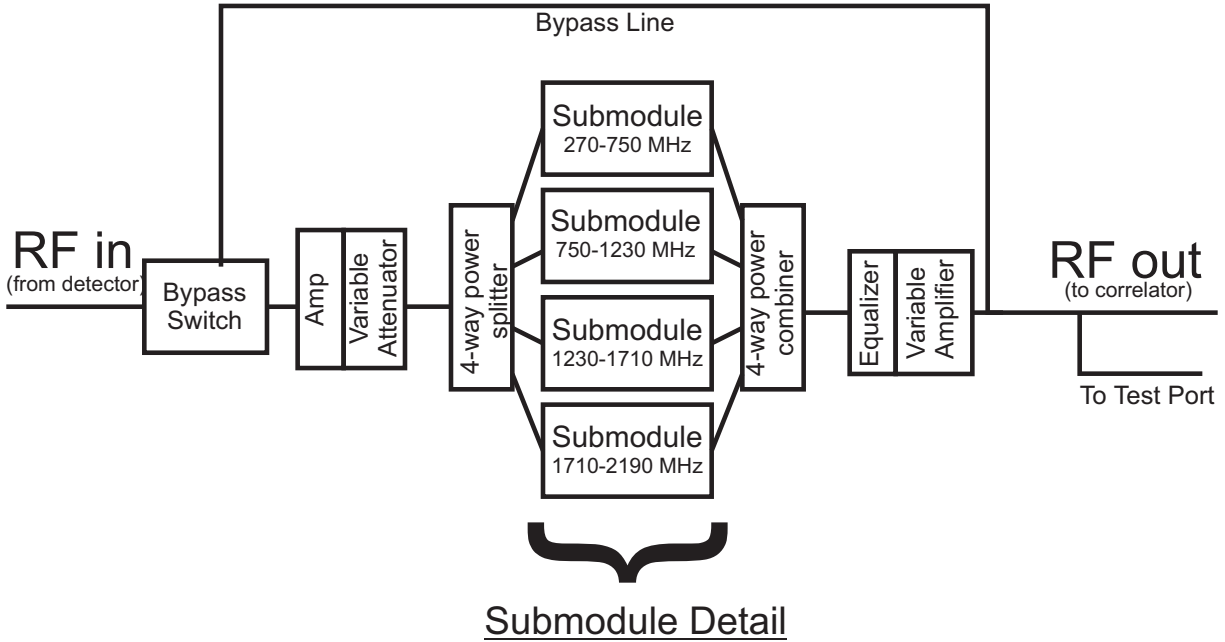


Fig. 2.— This figure shows a block diagram of one of the filterbank modules; there is one per telescope.

Onboard memory allows the storage of two separate bandpass selections, which can be switched back and forth rapidly either by a computer-controlled chop signal or one from an external signal generator. This capability allows the measurement of both the narrow absorption line and the broad continuum on alternate chop cycles within an atmospheric coherence time, removing brightness fluctuations as a source of measurement uncertainty. Bandpass selection and gain/attenuator control can be accomplished via manual switching or through a computer interface. Presently, the filterbank bandpass and gain selections are made using a C-language program running on a Sun workstation interfaced with the main ISI control computer.

2.3. Performance

Figure 3 shows the transmission of the two filterbank modules of the completed filterbank. An ideal frequency response would be a flat transmission curve inside the allowed bandpass. However, a peak in the transmission occurs at overlapping band edges due to a design flaw in the individual filter bandpasses; see Monnier (1999) for further detail. The net effect of this mismatch is a slight degradation of the signal-to-noise ratio. This occurs because when the RF is finally detected in a diode, the signal adds up coherently as a function of frequency, while the noise adds up incoherently. In order to accurately estimate the effect on the SNR, the phase response of the system must also be characterized. A network analyzer has been used to measure the relative phase delay for RF signals propagating through the two modules of the filterbank. This “differential phase” response appears in figure 4 and shows that the phase is matched to $\pm 10^\circ$ over 80% of the bandpass and is always within 20° . Using this information, calculation (based on Eq. (6.36) in Thompson, Moran, & Swenson [1986]) shows that the filterbank gain ripple only decreases the signal-to-noise ratio by $\sim 10\%$ over most of the bandpass. Further discussion of the SNR degradation as a function of frequency can be found in Monnier (1999).

In order to confirm these calculations, signal-to-noise ratio measurements were made at the telescope while observing a calibration hotbody source (373 K). The results can be found in figure 5. The SNR was measured for a series of bandpass widths throughout the full frequency range. There are two major conclusions that can be drawn from these measurements. First, the signal-to-noise ratio has the expected behavior as a function of bandwidth ($\text{SNR} \propto \sqrt{\text{Bandwidth}}$). Secondly, the SNR of the filterbank, when extrapolated to the effective bandwidth of normal ISI system (~ 2300 MHz), is $\sim 10\%$ low (expected $\text{SNR} \sim 500$), confirming the theoretical expectation that the gain ripple causes only a modest loss in SNR.

3. Observing Methodology

The filterbank observing methodology described in this section allows a precise and accurate *relative* measurement of the infrared power in two bandpasses. The first, Bandpass 0 (BP0), is

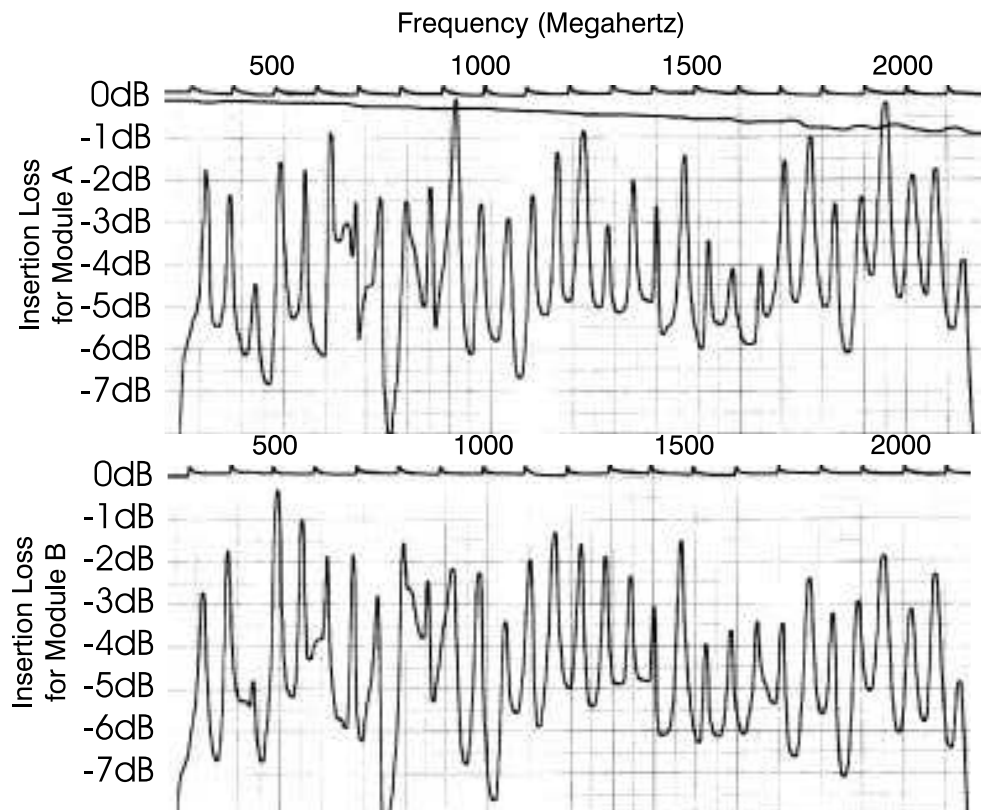


Fig. 3.— This figure shows the filterbank transmission (or insertion loss) as a function of frequency for both filterbank modules. The two horizontal lines with tick marks define the frequency scale in steps of 100 MHz. The nearly straight line with small slope near the top of the figure is the transmission of the cables connecting to the filterbank modules. The top curve (with the large ripple) corresponds to module A (plus connecting cables) used in telescope 1, while the bottom curve is the frequency response of module B used in telescope 2. Ideally these spectra should be flat, but improper overlap of neighboring filter bandpasses causes a ± 2.5 dB bandpass ripple (see §2.3).

Differential Phase Module A - Module B

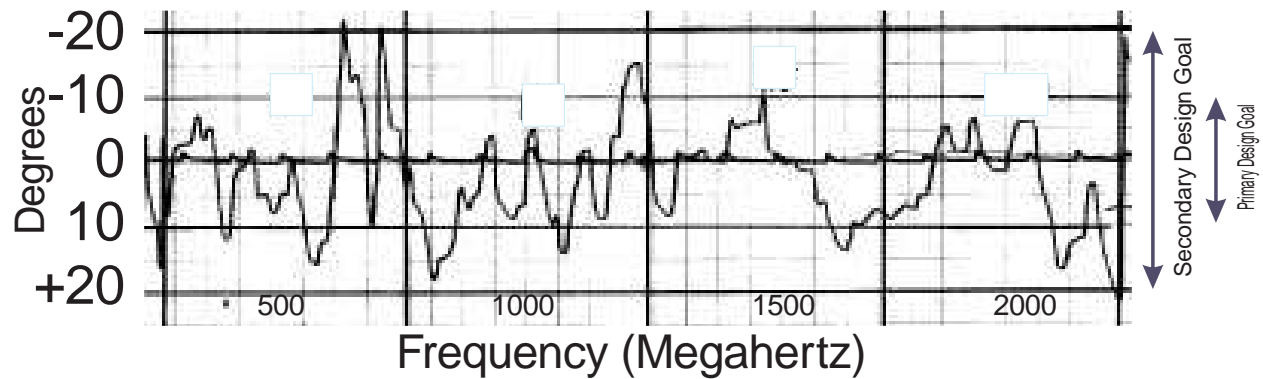


Fig. 4.— This figure shows the relative phase response of the two filterbank modules as a function of frequency. The bandpasses are matched to within 10° over 80% of the bandwidth, and always within 20° .

usually only a few filters wide (to match the absorption line width) while the second, Bandpass 1 (BP1), is typically much larger (to make an accurate measurement of the continuum). The filterbank switches rapidly between these two bandpasses in order to calibrate signal fluctuations due to seeing and telescope guiding changes. This observing strategy makes the ratio of IR power in BP0 to BP1 insensitive to such sources of fluctuations.

Determining the final calibrated ratio of infrared power in BP0 compared to BP1 requires 4 nested levels of comparison or chopping (sometimes 5), all easily controlled through a combination of hardware and software.

1. The sky signal is chopped at 150 Hz against a cold load to measure the infrared signal from the sky and minimize the effect of low frequency noise in the detection system.
2. The filterbank switches between BP0 and BP1 at 2.0833 Hz in order to calibrate out seeing and guiding changes.
3. The telescope nods $5''$ on either side of the star every 15 seconds to measure the changing thermal background of the atmosphere and telescope optics.
4. The flat spectrum of the hotbody source (373 K) is observed every 5 minutes to measure the overall (frequency-dependent) gain of the ISI system, precisely calibrating the IR power ratios in BP0 to BP1.
5. When using lasing transitions of the $^{12}\text{CO}_2$ molecule, a final calibration is made for telluric absorption of $^{12}\text{CO}_2$. This is done by repeating these IR power ratio measurements on the star but using a nearby transition of the CO_2 laser local oscillators, one which has no known molecular line coincidences within the filterbank's bandpass.

IR total power data taken in the above manner are analyzed using an Interactive Data Language (IDL) reduction package which automatically separates out the various signals and returns a calibrated IR power ratio of BP0 with respect to BP1.

4. Spectroscopy Results

As previously emphasized, the lack of multiplexed readouts makes the acquisition of full-bandwidth, high resolution spectra very time consuming. Hence, a series of strategic observations were planned to robustly test the experimental methodology and confirm calibration reliability. A deep and broad CO_2 absorption line of the Martian atmosphere and a single NH_3 absorption line of IRC +10216 were observed for these purposes, with results described below.

4.1. Mars

Deep absorption lines of Mars have previously been measured with a heterodyne spectrometer using a CO₂ laser as a local oscillator by Betz (1977). The mid-infrared spectrum of Mars arises from thermal emission of the warm surface, heated by the Sun. Since the atmosphere of Mars is composed largely of ¹²CO₂, deep absorption lines are formed when viewing the surface through this molecular blanket. Mars is roughly as bright as IRC +10216, the brightest stellar mid-infrared source, and its pronounced spectral features present an ideal test case for calibration and checks of observing methodology.

Mars was observed on 1996 November 08 (UT), with the ISI lasers tuned to the P(16) transition of ¹²C¹⁶O₂ at 10.55 μm. Combinations of 4 consecutive filters ($\Delta\nu = 240$ MHz) were observed across the entire ISI bandwidth to map out the spectral shape of the ¹²C¹⁶O₂ P(16) absorption in the atmospheres of Mars and the Earth. In each case, the narrow 4-filter set was compared to the full-bandwidth of the filterbank by frequency switching at 2.0833 Hz ($\tau=480$ ms) (see §3) and integrating for ~5 minutes. Figure 6 (top panel) shows the measured IR power in each of the 4-filter bandpasses relative to the average of the entire continuum. The presence of the Martian CO₂ line near 1400 MHz is superimposed on a shallower, broader absorption feature attributed to the telluric absorption. Since the ISI is not able to separate the upper and lower sidebands, the ~50% double-sideband depth of the Mars absorption line corresponds to nearly 100% absorption in a single sideband. This “folded” spectrum can be decomposed into the two sidebands by use of a model for the spectral shape.

After decomposition, the double-sideband spectrum in figure 6 (top panel) is represented by a superposition of two Gaussian absorption features on a flat continuum. The center of one Gaussian is fixed at 0 MHz to fit telluric absorption, while the other Gaussian center is left free to fit the location of the Mars absorption core. The fitting procedure compensates for the relatively low spectral resolution (240 MHz) by smoothing the candidate double-sideband spectrum before folding and comparing to the data. The result of this fit shown in the bottom panel of figure 6 is in good agreement with expectations. The line center of the Mars line can be predicted based on the relative velocity of Mars with respect to Earth along the our line of sight. NASA ephemerides predict a relative velocity of -14.54 km s⁻¹ on the date of observation. The corresponding Doppler shift is 1378 MHz at 10.55 μm, which is good agreement with the best-fitted center of 1380 MHz.

4.2. IRC +10216: NH₃ aQ(2,2)

The observation of Mars convincingly demonstrated spectral line observations with the ISI and this filterbank. However, for observation of narrow stellar lines, one must *very* precisely compensate for the orbital motion of the Earth (doppler shifts due to the Earth’s rotation are slightly less than the resolution of the filterbank and are neglected). Software to predict molecular line doppler shifts which had previously been used for the heterodyne measurements of AGB stars in the 1980s

(Goldhaber 1988) was provided by Dr. Betz.

Two test observations of IRC +10216, separated by two weeks, were made in Spring of 1997. The observations were separated in time to allow the Earth to move along its orbit enough for a detectable shift in the line position to occur. Furthermore, since the chosen line had been previously observed by Goldhaber (1988), these observations would test whether the line depth has remained constant over the last decade. Both observations employed combinations of two filters which resulted in a spectral resolution of 120 MHz, just small enough to resolve the line as it appeared in Goldhaber ([1988] $\sigma \sim 150$ MHz). Figure 7 shows the results of these observations from May and June 1997.

Gaussian absorption features, smoothed to the 120 MHz resolution of this observation, were fitted to the data and the line center frequencies determined. Table 2 shows the observed line center locations and the theoretical predictions. The agreement is excellent and justifies interferometric observations in the cores of previously observed lines with confidence in the calculations. The line detection in May was only marginal, but the movement of the absorption core is clear. While poorly determined, the apparent line widths and depths are consistent with the previous measurements of Goldhaber (1988).

4.3. Final calibration check

One further set of tests was performed to determine the accuracy of the IR power ratio measurements. The infrared power ratio in two different filterbank bandpasses, denoted by Bandpass 0 and Bandpass 1, was measured in Fall 1998 on 8 separate occasions while observing featureless stellar spectra (i.e, no known line coincidences). The average IR power of the full dataset in Bandpass 0 compared to Bandpass 1 was 0.996 ± 0.005 , consistent with unity.

Table 2. Test of software which calculates Doppler shifts of celestial spectral lines: NH_3 aQ(2,2) around IRC +10216

Date (UT)	Observed Absorption Core Location (MHz)	Predicted Absorption Core Location (MHz)
1997 May 28-29	1117 ± 8	1124
1997 June 11-12	1299 ± 35	1326

5. Interferometry on Spectral Lines: Methodology

Previous sections discussed the methodology of taking infrared power measurements on and off of a spectral line. However to perform interferometry, the fringe signal must be measured on and off the line as well. Measurements of the fringe power ratio on and off a spectral line can be combined with the IR power ratio measurements to yield the *visibility* ratio on and off the line, according to the formula (Hale *et al.* 2000):

$$\text{Visibility Ratio} = \sqrt{\frac{\text{Fringe Power Ratio}}{\text{IR Power Ratio Telescope 1} \times \text{IR Power Ratio Telescope 2}}} \quad (1)$$

This section will detail the methodology to obtain a well-calibrated fringe power ratio using the ISI filterbank system.

5.1. Frequency switching (bandpass chopping)

As with the IR power ratio, for fringe power measurement the ISI filterbank is preset so that a narrow bandpass is selected to coincide with the core of a molecular absorption feature; this bandpass is referred to as Bandpass 0 (BP0). A broad bandpass away from the absorption core, Bandpass 1 (BP1), is selected as a reference. BP1 is generally much larger than BP0 so that shot noise in the BP0 measurement is the dominant noise term in the ratio of BP0 to BP1. A switching signal, generated and recorded by the real-time computer, is used to chop between these two bandpasses.

The frequency switching rate is adjustable and can be slowed to take advantage of good seeing conditions. In ordinary seeing conditions, a switching period of 240 ms is used, hence each bandpass is observed for blocks of 120 ms at a time. Even during poor atmospheric conditions, this provides for accurate calibration of fringe amplitudes and (relative) phase, allowing shot-noise (in BP0) to dominate the measurement error of the fringe power. For observing nights with excellent seeing, a slower frequency switching rate allows longer coherent integration due to the longer atmospheric coherence time. In these cases, a 480 ms switching period was typically used.

For observations of an absorption line, the local oscillators were tuned to the appropriate lasing transition to bring the target molecular transition into the RF bandpass of the ISI detectors. Frequency switching was initiated and the correlator output voltage recorded (at 500 Hz) for an observation lasting approximately 5 minutes.

5.2. Delay line gain correction

As with any interferometer, the ISI uses a variable “delay line” to compensate for the changing geometric delay of the light coming from a source moving across the sky. While an automatic gain

control circuit has been implemented in the delay line to keep the average transmission constant as the delay length changes, the spectral shape of the transmission does not remain precisely constant. The frequency-dependent transmission (or “gain”) of the delay line can change by 5-10% over the course of a few minute observation, with a direct dependence on the specific length of delay in place. As can be seen in figure 1, the filterbank is located in the RF chain *after* the delay line and hence these changes corrupt the desired measurement of the fringe amplitude ratio on and off of the spectral line. On the 4m baseline, which was used for most of the filterbank observations, the delay line changed every 20-60 seconds, depending on the source elevation. The associated spectral changes had to be calibrated in order to achieve accurate calibration of the fringe amplitude ratio of BP0 to BP1.

A real-time module was written and incorporated into the ISI delay line software in the control computer for this purpose. When activated, this code instructs the data acquisition program to record into a file the exact time and settings of the delay line during an observation. After each ~ 5 -minute measurement, the frequency dependent gain changes of the delay line were immediately calibrated. This was done by observing a known flat continuum source (the ISI hotbody source at 373 K) and measuring the IR power in BP0 and BP1 while cycling through the just-used delay line settings. While this method corrects for variations in the gain amplitude of the delay line, it does not correct possible phase mismatches which, if more than $\sim 20^\circ$, cause residual miscalibration in the fringe amplitude in BP0 with respect to BP1. Calibration of this effect is discussed in the next section.

5.3. Correlator drifts/LO switching

Extensive engineering observations during Fall 1997 and Spring 1998 revealed that the spectral response of the fringe measurement, or correlator circuitry, showed drifts on the time-scale of 0.5 hr, unrelated to the delay line settings. Despite significant engineering efforts, the source of these variations could not be controlled and one additional calibration procedure was adopted. Observations of a stellar source with a featureless spectrum were required for an absolute calibration of the fringe amplitude ratio on and off of a spectral line (BP0/BP1). After each 5-minute observation on the target spectral region using the appropriate laser LO line, the LOs were adjusted to a neighboring lasing transition and the process repeated. Hence interleaved observations were obtained under identical conditions except for the LO wavelength (which differed by $\sim 0.015\mu\text{m}$). The true ratio of fringe amplitude in BP0 to BP1 is then the BP0/BP1 ratio at the target LO wavelength, divided by the BP0/BP1 ratio at the calibration LO wavelength. This method (“LO switching”), while involving much off-source integration and repeated adjustments of the laser grating in order to change the laser frequency to the alternating transitions, is extremely robust, and has no known systematic biases.

5.4. Software for analysis of fringe data

Custom software written in IDL was used to read the recorded correlator voltage and bandpass-switching signals. This software took a power spectrum of each separate (usually 120 ms) block of fringe data for BP0 and BP1. The fringe power was measured around the fringe frequency (100 Hz) and the broadband noise signal was subtracted by sampling symmetric frequency bins ~ 20 Hz on either side of the main peak. Careful measurements during the engineering phase of the filterbank commissioning established the noise power spectrum after the correlator circuit to be linear with frequency around 100 Hz to within 0.5%. Data for each delay line setting were then collated and separately calibrated.

The mean and standard deviation of the fringe power in each bandpass and for each delay line setting were then determined by a simple bootstrap analysis (see Monnier [1999] for more detail). In addition, the fringe phase in BP0 can be subtracted from that measured in BP1. The frequency switching was rapid enough to eliminate atmospheric variations, essentially “freezing” the atmosphere, and the relative fringe phase in BP0 with respect to BP1 can hence be properly averaged (in the complex plane), a form of “phase-referencing.” After a total of a few nights of observing time on IRC +10216 using a narrow bandpass of about 180 MHz ($\Delta\lambda \sim 0.00007\mu\text{m}$), the visibility amplitude ratio of BP0 to BP1 was measured to a precision of $\sim 1\%$ and the relative fringe phase to less than a few degrees. The first interferometric results on spectral lines are presented in Paper III of this series.

6. Conclusions

An RF filterbank has been constructed and used with the ISI interferometer. The ISI filterbank functions well as a spectrometer, although the data rate is low. The filterbank system was not designed to be an efficient spectrometer, but rather to be an effective first-generation tool to harness the spectral resolving power of the ISI for interferometry. The observations presented here confirm the ability of the ISI to do such work, and an observing methodology for combining interferometric observing with filterbank observation has been outlined. This methodology has been used successfully for observing fringe visibilities on and off of a number of molecular absorption lines. Preliminary results are discussed in Monnier (1999), and a more complete analysis follows in Papers II and III of this series.

This new capability of the ISI has so far been used to measure the location of molecular formation zones for NH_3 and SiH_4 around the carbon star IRC +10216 and NH_3 around the red supergiant VY CMa. However, strong spectral absorption features of these same molecules could also be investigated for IRC +10420, *o* Cet, and NML Cyg, whose line depths and shapes have already been measured (McLaren & Betz 1980; Betz & Goldhaber 1985; Goldhaber 1988). Measurements of angular diameters of red supergiants and Miras on and off their recently discovered mid-infrared water lines (Jennings & Sada 1998) is also potentially rewarding. These lines are

thought to form in the stellar photosphere and may affect the interpretation of previous angular diameter measurements. The use of high spatial and spectral resolution line observations in between water lines could potentially allow the “true” continuum diameters to be measured, uncorrupted by line blanketing. Lastly, fine structure and recombination lines around some emission-line stars (e.g., MWC 349, Quirrenbach et al. 1997) can be observed using the CO₂ local oscillators, and could make unique measurements of the emitting regions.

While the potential for interesting new results is rich, the non-multiplexed output of this particular filterbank system makes it very difficult to observe new sources in detail when the spectral line profiles have not been previously measured by a multiplexing spectrometer. The lines around some sources (*o* Ceti, for instance) have been observed to change in time, and new spectra are essential for interpreting additional interferometric line data.

We want to recognize the computer programming of Manfred Bester and Carl Lionberger which was essential for the filterbank to interface with the ISI control system. This work is a part of a long-standing interferometry program at U.C. Berkeley, supported by the National Science Foundation (Grant AST-9221105, AST-9321289, and AST-9731625) and by the Office of Naval Research (OCNR N00014-89-J-1583).

REFERENCES

- Bester, M., Danchi, W. C., Hale, D., Townes, C. H., Degiacomi, C. G., Mekarnia, D. & Geballe, T. R. 1996, ApJ, 463, 336
- Betz, A. L., Johnson, M. A., McLaren, R. A. & Sutton, E. C. 1976, ApJ, 208, L141
- Betz, A. L. 1977, University of California at Berkeley, PhD Dissertation
- Betz, A. L. & Goldhaber, D. M. 1985, in Mass Loss from Red Giants, ed. M. Morris & B. Zuckerman (Dordrecht: Reidel), 83
- Danchi, W. C., Bester, M., Degiacomi, C. G., Greenhill, L. J. & Townes, C. H. 1994, AJ, 107, 1469
- Goldhaber, D. M. 1988, University of California at Berkeley, PhD Dissertation
- Hale, D. D. S., et al. 2000, ApJ, Submitted
- Holler, C. 1999, Ludwig-Maximilians-Universitaet, Master’s Thesis
- Isaak, K., Harris, A. I. & Zmuidzinas, J. 1999, in Highly Redshifted Radio Lines, ASP Conf. Series Vol. 156, Ed. by C. L. Carilli, S. J. E. Radford, K. M. Menten, & G. I. Langston, p. 86
- Jennings, Donald E. & Sada, Pedro V. 1998, Science, 279, 844

Lipman, E. A. 1998, University of California at Berkeley, PhD Dissertation

McLaren, R. A. & Betz, A. L. 1980, ApJ, 240, L159

Monnier, J. D. 1999, University of California at Berkeley, PhD Dissertation

Quirrenbach, A., Thum, C., Martin-Pintado, J. & Matthews, H. E. 1997, BAAS, 191, 4719

Thompson, A. Richard, Moran, James M. & Swenson, George W. 1986, *Interferometry and synthesis in radio astronomy*, Wiley-Interscience: New York

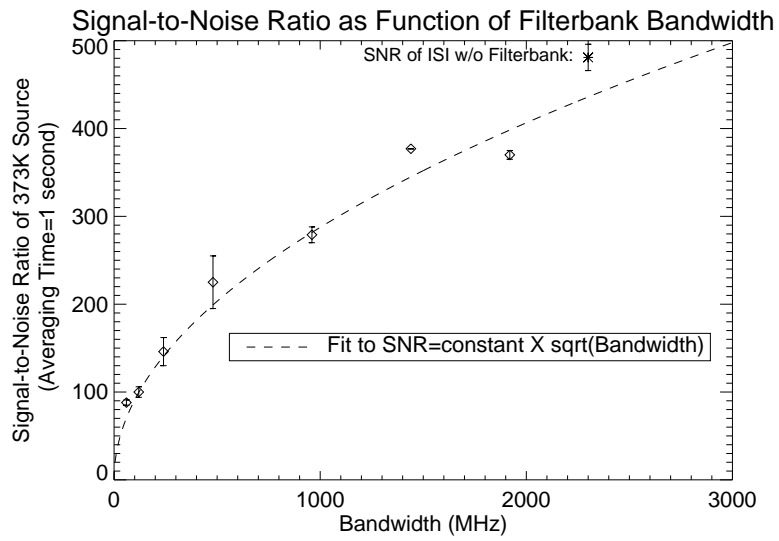


Fig. 5.— A plot of the signal-to-noise ratio for observations of a 373K blackbody with and without the filterbank. This confirms that the system is shot-noise limited and that the filterbank degrades the sensitivity by about 10% as expected.

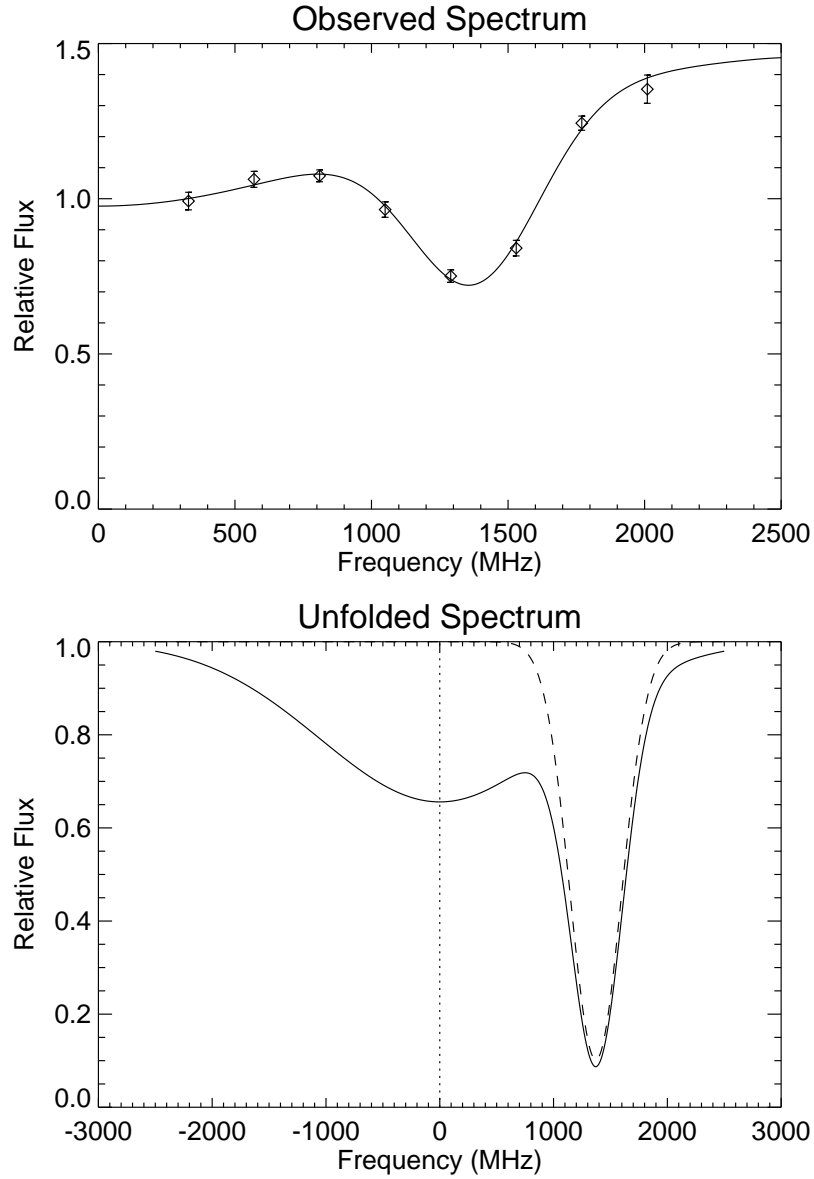


Fig. 6.— *Top Panel:* Mars observation of P(16) transition of $^{12}\text{CO}_2$ on 1996 Nov 8. *Bottom Panel:* A two-gaussian model of the (unfolded) double-sideband spectrum. The wide gaussian centered at 0 frequency comes from telluric absorption, while the narrow, shifted feature is from the atmosphere of Mars itself. The relative velocity of Mars during this observation was -14.54 km/s (1378 MHz at $10.55 \mu\text{m}$).

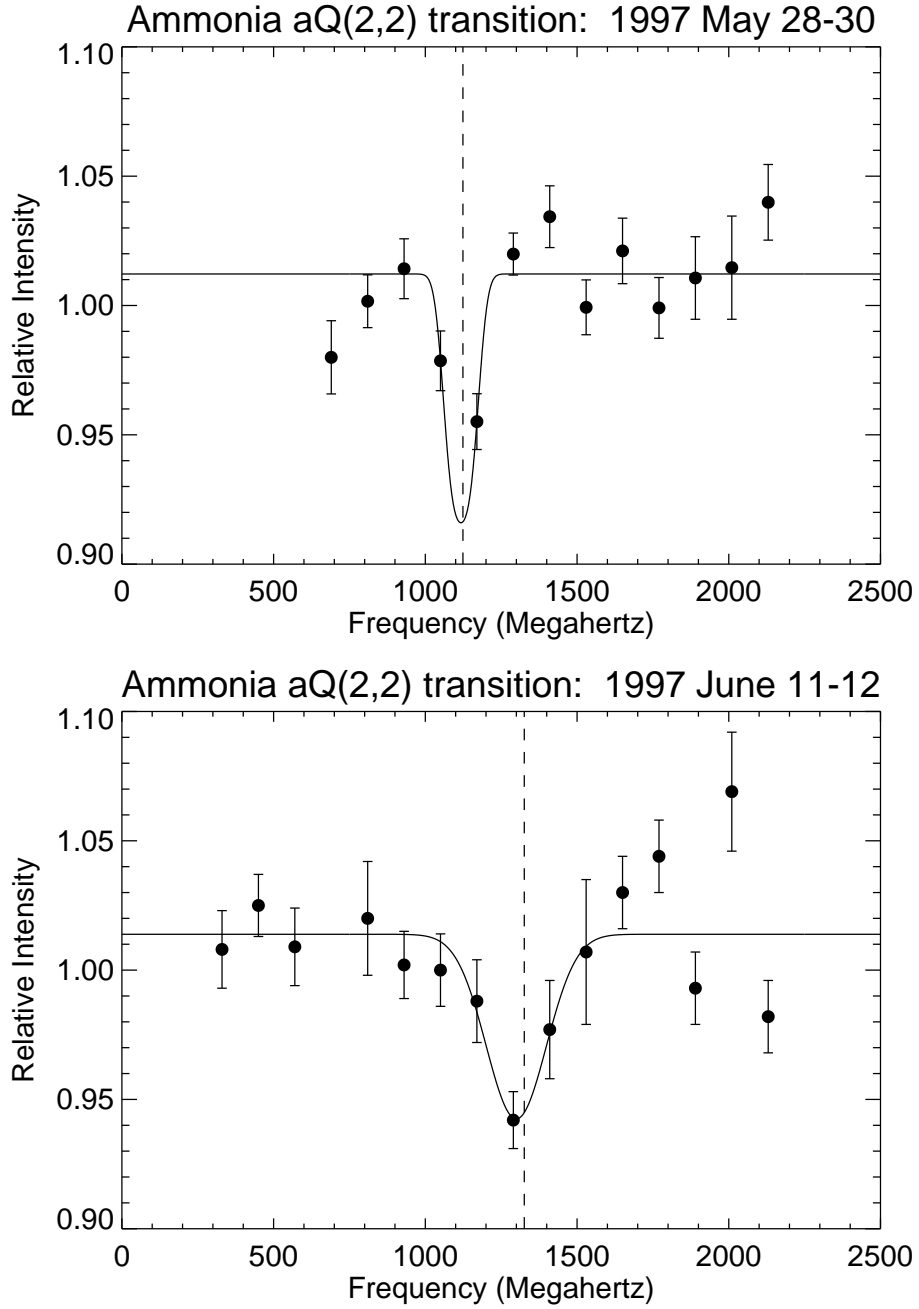


Fig. 7.— *Top Panel:* Observation of aQ(2,2) transition of NH_3 around IRC +10216 on 1997 May 28-30 *Bottom Panel:* Observation of aQ(2,2) transition of NH_3 around IRC +10216 on 1997 June 11-12. Single gaussian fits to the absorption profiles are shown. The vertical dashed line in each panel marks the predicted location of the absorption core, based on previous observations. Due to the Earth's orbital motion, there is a frequency shift between observations which is clearly detected.